The role of Nrf2 in acute and chronic muscle injury

Iwona Bronisz-Budzyńska
Uniwersytet Jagiellonski w Krakowie
Magdalena Kozakowska
Uniwersytet Jagiellonski w Krakowie
Agnieszka Łoboda
Uniwersytet Jagiellonski w Krakowie
Józef Dulak (jozef.dulak@uj.edu.pl)
Uniwersytet Jagiellonski w Krakowie https://orcid.org/0000-0001-5687-0839

Research

Keywords: Nrf2, Duchenne muscular dystrophy, skeletal muscle, satellite cells, mdx, inflammation, regeneration, cardiotoxin-induced injury

Posted Date: April 20th, 2020

DOI: https://doi.org/10.21203/rs.3.rs-23184/v1

Version of Record: A version of this preprint was published on December 8th, 2020. See the published version at https://doi.org/10.1186/s13395-020-00255-0.

Abstract

The nuclear factor erythroid 2-related factor (Nrf2) is considered as a master cytoprotective factor regulating the expression of genes coding for anti-oxidant, anti-inflammatory, and detoxifying proteins. The role of Nrf2 in the pathophysiology of skeletal muscles has been evaluated in different experimental models, however, due to inconsistent data, we aimed to investigate how Nrf2 transcriptional deficiency ($Nrf2^{tKO}$) affects muscle functions both in acute and chronic injury. The acute muscle damage was induced in mice of two genotypes – WT and $Nrf2^{tKO}$ mice by cardiotoxin (CTX) injection. To investigate the role of Nrf2 in chronic muscle pathology, *mdx* mice that share genetic, biochemical, and histopathological features with Duchenne muscular dystrophy (DMD) were crossed with mice lacking transcriptionally active Nrf2 and double knockouts (*mdx*/$Nrf2^{tKO}$) were generated.

We have observed slightly increased muscle degeneration and delayed regeneration in $Nrf2^{tKO}$ mice after CTX treatment. Nevertheless, transcriptional ablation of Nrf2 in *mdx* mice did not significantly aggravate the most deleterious pathological hallmarks of DMD such as degeneration, inflammation, fibrotic scar formation, and decreased angiogenesis, as well as the number and proliferation of satellite cells.

In conclusion, our analyses in both acute and chronic injury mouse models have revealed no significant influence of Nrf2 transcriptional deficiency on skeletal muscle regeneration and function.

Background

Duchenne muscular dystrophy (DMD) is the most common form of muscular dystrophies (1), which affects one in 5000–6000 male births (2). DMD is the lethal X-chromosome linked recessive genetic neuromuscular disorder, caused by mutations in the gene encoding dystrophin (1). Dystrophin deficiency leads to progressive muscle weakness, severe muscular atrophy, cardiomyopathy, and respiratory impairments, the two latter being the leading causes of mortality among patients with DMD (2). Dystrophin, a cytoskeletal protein, is a major structural element of the dystrophin-glycoprotein complex (DGC), which is responsible for maintaining cellular integrity by linking the sarcolemmal and actin cytoskeleton to the extracellular matrix component laminin (3). The loss of dystrophin disrupts the complex resulting in sarcolemmal instability, that makes cells more susceptible to damage and leads to necrosis of muscle fibers (3). Consequently, it results in the activation of the innate immune system, excessive inflammatory response and increased oxidative stress (4).

In the early stage of the inflammatory response muscles are infiltrated by neutrophils and pro-inflammatory, phagocytic M1-like macrophages. which are a rich source of Th1 cytokines, that promote the activation and chemotaxis of myeloid cells to damaged tissue. Moreover, cytokines affect proliferation, migration, and differentiation of muscle satellite cells (SCs), progenitors of mature skeletal muscle. Subsequently, the recruitment of anti-inflammatory and pro-regenerative subpopulation of M2-like macrophages is observed (5). In addition to macrophages and neutrophils, other inflammatory cells, including T-lymphocytes (cytotoxic, helper and regulatory) may contribute to disease progression (6,7).

Subsequently, injury leads to muscle regeneration, a process that depends on activation and proliferation of SCs and their differentiation into myotubes and later on regenerating myofibres that are centrally nucleated and exhibit expression of embryonic myosin heavy chain (eMyHC) isoform. Eventually, in chronic injury, the continuous cycles of myofiber degeneration and regeneration induce exhaustion of SCs and substitution of muscle with fibroadipose tissue (4). Additionally, oxidative stress with elevated production of reactive oxygen species (ROS) have been proposed as important contributors in the pathogenesis of the DMD in humans (8) and *mdx* mice (murine model of DMD) (9).

Recently, we have shown that expression of heme oxygenase–1 (HO–1, encoded by *Hmox1),,* anti-inflammatory and cytoprotective enzyme, is strongly elevated in muscles of *mdx* mice and muscle biopsies of DMD patients. Genetic loss of HO–1 exacerbates not only dystrophic phenotype and inflammation in *mdx* mice (10), but aggravates also skeletal muscle injury in acute muscle damage model, i.e. following cardiotoxin (CTX) induced injection (11). Expression of *Hmox1* is regulated, among others, by the redox-sensitive nuclear factor erythroid 2-related factor 2 (Nrf2, encoded by *Nfe2l2* gene) belonging to Cap 'n' collar (Cnc)-bZIP (basic leucine zipper) family of transcription factors (12). Nrf2 plays a cytoprotective role as a master regulator of genes encoding oxidative stress response and phase II detoxifying proteins by interacting with ARE (Antioxidant Response Element) sequence. Under normal circumstances, Nrf2 is sequestered in the cytoplasm by Keap1 (Kelch-like ECH-associating protein 1) through the Nrf2-Keap1 complex, which suppresses Nrf2 activity by targeting it for ubiquitination and degradation. In stressful conditions, Nrf2 dissociates from Keap1, translocates into the nucleus and induces the expression of target genes (13). The role of Nrf2 in skeletal muscle aging and adaptations to exercise through the regulation of mitochondrial function, maintaining the cellular redox balance, control of oxidative stress, influencing apoptotic signaling and providing proper contractile properties has been demonstrated (14,15). Although the involvement of Nrf2 in DMD progression has been suggested (16–19), the possible protective mechanisms were not fully discovered. Therefore, we aimed to evaluate the impact of Nrf2 transcriptional deficiency on the acute muscle damage caused by CTX injection and chronic injury using a murine model of DMD—*mdx* mice.

Methods

Animal models

All animal procedures and experiments were performed in accordance with national and European legislation, after approval by the 1st and 2nd Institutional Animal Care and Use Committee (IACUC) in Kraków, Poland (approval number: 66/2013 and 199/2018). Mice were kept in specific-pathogen-free (SPF) conditions with water and food available *ad libitum* under controlled temperature and humidity and 14 h:10 h light:dark cycles.

Mdx mice (C57BL/10ScSn-*Dmd*^{mdx}/J) and control mice (C57BL/10ScSnJ, WT) were purchased from the Jackson Laboratory. The mice with disrupted *Nfe2l2* gene on C57Bl/6J background, originally developed by Prof. Yamamoto (20) and further demonstrated by us to be a transcriptional knockout (tKO), as the

Keap-binding domain is present (21), were bred in our animal facility from the mice originally provided by Prof. Antonio Cuadrado (22). To generate Nrf2^{tKO}*mdx* (mice deficient for both dystrophin and transcriptionally active Nrf2), homozygous Nrf2^{tKO} male mice were bred to homozygous *Dmd*$^{mdx/mdx}$ female mice, to generate Nrf2$^{+/-}$Dmd$^{mdx/+}$ female mice or Nrf2$^{+/-}$Dmd$^{mdx/Y}$ male mice, which were bred together to obtain Nrf2^{tKO}*mdx* mice at mixed background C57BL/10ScSn and C57BL/6J.

In the experiments 10-12-week-old male littermates or age-matched mice from generation F2 to F5 were used. Accordingly, the double knockout animals lacking both dystrophin and Nrf2 expression (Nrf2^{tKO}Dmd$^{mdx/Y}$) were compared to their *mdx* littermates (Nrf2$^{+/+}$Dmd$^{mdx/Y}$). Additionally, *mdx* mice were analysed vs. WT (Nrf2$^{+/+}$Dmd$^{+/Y}$) mice and the comparison of Nrf2^{tKO} (Nrf2^{tKO}Dmd$^{+/Y}$) mice vs. WT mice was studied as well.

The generation of double knockouts was hence done accordingly to other studies in which *mdx* mice were crossed with relevant knockouts (10,23–26). Genotyping of animals was performed by PCR on the DNA isolated from the tails. For tissue collection, mice were sacrificed by CO_2 exposure.

CTX-induced injury

Male and female C57BL/6J (WT and Nrf2^{tKO}) mice at 8-15-weeks of age were used for the myoinjury experiment. Hind limbs of mice were shaved and gastrocnemius muscles (GM) were injected with 25 µl of 20 µmol/L CTX (Sigma-Aldrich), while control mice were injected with saline. Animals were provided with analgesia (50 µl, 0.03 mg/ml buprenorphine) after injection and in the next 2 days. Mice were euthanized on the 1st, 3rd, 7th, 14th, and 28th day after CTX injury. Subsequently, plasma was taken and GM were harvested for further analyses.

Treadmill test

The treadmill test was performed as previously described (10,25) using the Exer-3/6 treadmill (Columbus Instruments).

Plasma creatine kinase (CK) and lactate dehydrogenase (LDH) measurement

Plasma was obtained by blood collection from *vena cava* to heparin-coated tubes followed by centrifugation at 1000 g for 10 minutes at 4ºC just before the terminal procedure and collection of GM. Activity of CK and LDH were measured using diagnostic Liquick Cor-CK and Liquick Cor-LDH kit, respectively (P.Z. CORMAY) following the manufacturer's instruction.

Histological analysis

GM were dissected, immediately fixed in 10% formalin, processed, embedded in paraffin and cut on 4 µm sections. Subsequently, sections were deparaffinized, rehydrated and subjected to histological stainings.

Hematoxylin and eosin staining (H&E, Sigma-Aldrich) was performed to visualize inflammation and regenerating myofibers according to standard protocols. For Masson's trichrome staining assessing collagen content (fibrosis evaluation), sections were fixed overnight in Bouin's solution and sequentially treated with biebrich scarlet-acid fuchsin, phosphotungstic acid/phosphomolybdic acid and aniline blue (Sigma-Aldrich, according to the vendor's instructions). Inflammation, regeneration, fibrosis, and degeneration scoring were done by a blinded observer not knowing the origin of samples (arbitrary units: 0–none, 1–mild, 2–mild-moderate, 3–moderate, 4–severe; described in details in (11)).

Immunohistofluorescent (IHF) stainings

GM were harvested and snap-frozen in optimal cutting temperature compound (OCT, Leica) in liquid nitrogen-chilled isopentane and stored at -80ºC until processed. Frozen tissues were cryosectioned (10 µm) using a cryostat (Leica) and placed on glass slides coated previously with poly-L-lysine (Sigma-Aldrich).

For evaluation of necrotic fibers (accumulating IgG and IgM) and regenerating fibers (positive for embryonic myosin chain, eMyHC), sections were blocked with 10% goat serum (Sigma-Aldrich), 5% bovine serum albumin (BSA, BioShop) and mouse-on-mouse (M.O.M.^{TM}, Vector Laboratories) for 1 h at room temperature, and incubated with rat anti-mouse laminin 2a (1:500; 4H8-2, Abcam) and mouse anti-mouse eMyHC (1:100, F1.652, DSHB) primary antibodies for 1 h at 37ºC. After three washes with PBS (5 minutes each), the sections were incubated with goat anti-rat Alexa Fluor 568 (1:1000, A-11077, Thermo Fisher Scientific and goat anti-mouse IgG/IgM/IgA Alexa Fluor 488 (1:50, A-10667, Thermo Fisher Scientific) secondary antibodies for 1 h at 37ºC. Paired-box 7 (Pax7) expression was checked on frozen cryosections fixed by 4% paraformaldehyde (Santa Cruz Biotechnology) and cold methanol (Avantor Performance Materials Poland S.A.). After antigen retrieval samples were blocked for 30 minutes with 2.5% BSA and for the next 30 minutes with M.O.M.^{TM}. Following two washes with PBS, sections were stained overnight at 4°C with mouse anti-mouse Pax7 (1:100, Pax7-c, DSHB) and rabbit anti-mouse laminin 2α (1:1000, L9393, Sigma-Aldrich) primary antibodies diluted in 0.1% BSA. Secondary stains were done using goat anti-mouse Alexa Fluor 488 (1:500, A11008, Thermo Fisher Scientific) and goat anti-rabbit Alexa Fluor 568 (1:500, A-11077, Thermo Fisher Scientific) secondary antibodies diluted in 0.1% BSA. Finally, sections were washed with PBS 3 x 5 minutes, during the last washing step nuclei were stained with Hoechst 33258 (10 µg/ml, Sigma-Aldrich) followed by mounting the slides with fluorescence mounting medium (Dako). Images were acquired using a fluorescent microscope (Leica DMI6000B) and analysed in ImageJ software. To analyse the level of necrosis or eMyHC expression number of necrotic or eMyHC-positive cells was counted in 8 fields of view or within all injured sites of GM in the experiments with CTX injection, at 100x magnification. The percentage of necrotic/eMyHC^{+} myofibers was calculated in relation to the total number of myofibers. The ratio of Pax7^{+} nuclei/myofiber was estimated by counting Pax7^{+} nuclei and myofibers in at least 10 fields of view at 200x magnification.

Gene expression analysis by quantitative real-time PCR

Harvested skeletal muscle tissues were stored in RNA*later* RNA Stabilization Solution (Invitrogen) at -80ºC until processed. GM from 12-week-old mice were used to isolate RNA by homogenization in 1 ml of Quiazol Total RNA Isolation Reagent (Qiagen) using TissueLyser (Qiagen), following the manufacturer's instructions. The concentration and quality of RNA were determined spectrophotometrically (NanoDrop, Thermo Fisher Scientific). To synthesize cDNA, the reverse transcription reaction was performed on 1 µg RNA using RevertAid reverse transcriptase (Thermo Fisher Scientific) or MystiCq® microRNA cDNA Synthesis Mix (Sigma-Aldrich). Quantitative PCR (qPCR) was performed with Applied Biosystems™ StepOnePlus Real-Time PCR (Thermo Fisher Scientific) in a mixture containing 1x concentrated SYBR Green PCR Master Mix (SYBR Green qPCR Kit, Sigma-Aldrich), 10 µmol/L forward and reverse primers and 10 ng cDNA. Sequences of primers recognizing murine genes are listed in Table 1 and muscle-specific murine microRNA in Table 2. Universal reverse primer for miRNAs quantitative RT-PCR was supplied by a vendor. The relative quantification of gene expression was quantified based on the comparative Ct (threshold cycle value) method. Gene expression levels were calculated by normalizing to the level of housekeeping gene *Eef2* or constitutive small nuclear RNA U6 in the case of microRNA.

Table 1. Sequences of primers used for RT-qPCR analysis.

gene name	forward primer	reverse primer
Col1a1	5'-CGATCCAGTACTCTCCGCTCTTCC-3'	5'-ACTACCGGGCCGATGATGCTAACG-3'
Eef2	5'-agaacatattattgctggcg-3'	5'-caacagggtcagatttcttg-3'
Il-1b	5'- CTGGTGTGTGACGTTCCCATTA -3'	5'- CCGACAGCACGAGGCTTT -3'
Il-6	5'-AAAGAGTTGTGCAATGGCAATTCT -3'	5'- AAGTGCATCATCGTTGTTCATACA -3'
Kdr	5'- CGGCCAAGTGATTGAGGCAG-3'	5'- ATGAGGGCTCGATGCTCGCT-3'
Myh3	5'-TCTAGCCGGATGGTGGTCC-3'	5'-GATTGTAGGAGCCACGAAA-3'
Myod1	5'-GCTGCCTTCTACGCACCTG-3'	5'-GCCGCTGTAATCCATCATGC-3'
Myog	5'-CAGTACATTGAGCGCCTACAG-3'	5'-GGACCGAACTCCAGTGCAT-3'
Tgfb1	5'-GGATACCAACTATTGCTTGAG-3'	5'-TGTCCAGGCTCCAAATATAG-3'
Vegfa	5'- ATGCGGATCAAACCTCACCAA-3'	5'- TTAACTCAAGCTGCCTCGCCT-3'

Table 2. Sequences of primers used for RT-qPCR analysis – microRNA.

microRNA name	forward primer
miR-1	5'- GCTGGAATGTAAAGAAG TATGTAT -3'
miR-133a/b	5'-TGGTCCCCTTCAACCAGCTGT -3'
miR-206	5'- TGGAATGTAAGGAAGTGTGTGG -3'
U6	5'- CGCAAGGATGACACGCAAATTC -3'

Analysis of mononucleated cell populations in skeletal muscles by flow cytometry

Samples for flow cytometry were prepared as previously described (10,11). Briefly, mice were euthanized and immediately perfused with saline containing 0.5 U/ml heparin through the left ventricle. Then, hind limbs muscles were excised, minced, and digested at 37°C for 45 minutes in a solution containing collagenase IV (5 mg/ml; Gibco; Invitrogen) and dispase (1.2 U/ml; Gibco; Invitrogen). Digested muscles were passed through 100 µm cell strainer, washed with PBS, pelleted after centrifugation, and

resuspended in PBS+2% fetal bovine serum. Samples were stained with the following antibodies: rat anti-mouse CD45-APC-eFluor780 (30-F11, eBioscience), rat anti-mouse CD31-PE (MEC 13.3, BD Bioscience), rat anti-mouse CD34-Alexa Fluor 700 (RAM 34, eBioscience), rat anti-mouse Ly6A/E-PE-Cy7 (Sca-1; D7, eBiosience), rat anti-mouse α7-integrin-PE (334908, R&D Systems) – to analyse muscle SCs; rat anti-mouse CD45-APC-eFluor780 (30-F11, eBioscience), rat anti-mouse CD11b-PE (M1/70, eBioscience), rat anti-mouse F4/80-APC (BM8, eBioscience), rat anti-mouse MHCII-PE-Cy7 (M5/114.15.2, BD Bioscience), rat anti-mouse CD206-PerCP/Cy5.5 (C068C2, BioLegend), rat anti-mouse Ly6C-AlexaFluor488 (HK 1.4, BD Biosciences), rat anti-mouse Ly6G-PE (1A8, BioLegend) – to analyse macrophages and monocytes; rat anti-mouse CD45-APC-eFluor780 (30-F11, eBioscience), hamster anti-mouse CD3e-PE-Cy7 (145-2C11, eBioscience), mouse anti-mouse NK1.1-FITC (PK 136, BioLegend), rat anti-mouse CD4-PerCP/Cy5.5 (RM 4-5, BD Biosciences), rat anti-mouse CD8a-Alexa Fluor 700 (53-6.7, BioLegend), rat anti-mouse CD25-PE (PC61, BD Bioscience), rat anti-mouse FoxP3-APC (FJK-16s, eBioscience) – to analyze lymphocyte populations and NK-cells. Before flow cytometry analysis all cells were additionally stained with Hoechst 33342 (10 µg/ml). The proliferation of SCs was determined based on increased Hoechst staining. Data were acquired with a Fortessa flow cytometer (BD Biosciences) and were analysed using FACSDiva software (BD Biosciences).

Protein isolation

Total protein was isolated from snap-frozen GM by homogenization in lysis buffer – PBS containing inhibitors of proteinases (Roche) and 1% Triton X-100 (BioShop) using TissueLyser (Qiagen). Samples were then incubated on ice for 30 minutes, centrifuged (8 000 g, 10 minutes, 4°C), supernatants were collected, and stored at -80°C.

Protein analysis

To assess monocyte chemoattractant protein 1 (MCP-1) and vascular endothelial growth factor (VEGF) protein level, GM lysates were subjected to Luminex^{TM} measurement according to the manufacturer's instructions (Life Technologies) and the results were calculated as pg/mg of total protein.

Statistics

Data are presented as mean ± SEM and analysed with the unpaired two-tailed Student's t-test to determine differences between two groups or one-way ANOVA followed by Tukey's post-hoc test for multiple groups. $p \leq 0.05$ was considered as significant. Grubb's test was used to identify significant outliers, GraphPad Prism for statistical graphs and analyses. The information about the number of samples is indicated in the figure legend.

Results

Lack of transcriptionally active Nrf2 enhances skeletal muscle degeneration after CTX-induced injury

To analyse the effect of Nrf2 transcriptional deficiency during acute muscle damage, we examined inflammatory reaction and muscle degeneration as well as regeneration in the model of CTX-induced myoinjury. In Nrf2^{tKO} mice the level of muscle degeneration and inflammatory infiltration evaluated based on H&E staining (Fig. 1 A, B) was significantly higher in Nrf2^{tKO} mice on the 3rd day after muscle damage. Although the activity of CK (Fig. 1 C) was increased in Nrf2^{tKO} animals on day 1 after injection, a statistically significant difference between WT and Nrf2^{tKO} mice was not evident. On the other hand, the level of LDH (Fig. 1 D) was significantly elevated in mice of both genotypes, and additionally, it was much higher in Nrf2^{tKO} animals in comparison to WT on the 1st day after CTX injection. Moreover, *we have shown increased protein level of pro-inflammatory cytokine MCP-1 (Fig. 1 E) and mRNA level of Hmox1 (Fig. 1 F), Il1b (Fig. 8 G) and Il6 (Fig. 1 H) on the 1st day after CTX injection in both genotypes. Furthermore, IHF analysis of necrotic fibers on the 3rd day after myoinjury did not reveal differences between genotypes (Fig. 1 I, J).*

Muscle regeneration is not affected in the absence of transcriptionally active Nrf2 following CTX-induced injury

To assess the role of Nrf2 during muscle regeneration following the acute muscle injury caused by CTX injection, we examined the mRNA level of *Myh3* and the number of eMyHC^{+} myofibers. Following muscle damage we observed a higher level of *Myh3* in both WT and Nrf2^{tKO} animals on the 7th day after injury, however, there are no differences among genotypes in all time-points (Fig. 2 A). Accordingly, the number of eMyHC^{+} fibers was similar at the time of the peak of regeneration (7th day after injury) (Fig. 2 B, C).

Transcriptional deficiency of Nrf2 does not aggravate dystrophic phenotype in *mdx* mice

To investigate the role of Nrf2 in chronic muscle injury, we generated dystrophic mice lacking transcriptional activity of Nrf2 (Nrf2^{tKO}*mdx*). In order to determine whether the lack of Nrf2 can affect exercise performance, mice were subjected to a downhill treadmill run to exhaustion test. As shown by us (10) and others (25) previously, and confirmed in the present study, *mdx* mice were able to run a shorter distance than WT. However, we did not see any effect of transcriptional deficiency of Nrf2 on the running pattern. The exercise capacity of Nrf2^{tKO} animals was comparable to WT mice and Nrf2^{tKO}*mdx* mice run similar distance as *mdx* counterparts (Fig. 3 A). Body weight and GM mass significantly increased in *mdx* mice in comparison to healthy animals, while in Nrf2^{tKO}*mdx* no striking differences in body/GM mass compared with age-matched *mdx* mice were observed (Fig. 3 B, C).

Transcriptional knock-out of Nrf2 does not exacerbate degeneration in *mdx* mice

Muscle degeneration was evaluated based on the percentage of necrotic fibers in GM as well as the plasma level of CK and LDH, typical markers of muscle damage. Neither the number of necrotic fibers (Fig. 4 A, B) nor LDH (Fig. 4 C) and CK (Fig. 4 D) activity was changed between dystrophic mice lacking additionally Nrf2 and *mdx* animals, indicating a comparable level of muscle injury. As suspected, serum LDH and CK levels of *mdx* mice were elevated compared with those of WT mice (Fig. 4. C, D).

Lack of Nrf2 transcriptional activity does not aggravate the inflammatory reaction in dystrophic skeletal muscles

Since Nrf2 has been reported to be a master regulator of antioxidative responses and contributes to the anti-inflammatory process (27,28), we have assessed whether it can affect the inflammatory reaction in skeletal muscle in our experimental conditions. Analysis of H&E staining demonstrated that *mdx* mice lacking transcriptional activity of Nrf2 had a similar inflammation score to *mdx* mice (Fig. 5 A, B). Moreover, the expression of *Hmox1,* an anti-inflammatory factor shown by us to be up-regulated in dystrophic muscles (10), was again potently elevated in GM of *mdx* mice. However, it was the same in $Nrf2^{tKO}$*mdx* mice, indicating that Nrf2 transcriptional activity is dispensable for *Hmox1* induction in the muscles (Fig. 5 C).

For a broader view of inflammatory status, we have performed a comprehensive analysis of different leukocyte populations within skeletal muscles of hind limbs of mice of 4 genotypes using flow cytometry. *Mdx* mice demonstrated an elevated proportion of monocytes defined as $CD45^+F4/80^-CD11b^+Ly6C^+Ly6G^-$ cells. However, no further changes in the infiltration of this population into skeletal muscle were caused by Nrf2 transcriptional deficiency (Fig. 5 D, E). Similarly, the percentage of macrophages ($CD45^+F4/80^+CD11b^+$) was significantly higher in *mdx* mice in comparison to WT, however, it was not changed by the additional lack of Nrf2 transcriptional activity (Fig. 5 F, G). Due to the diverse functions of different subpopulations of macrophages (4), in the next step, we have investigated M1-like and M2-like macrophages, based on the gating strategy discriminating between MHCII and CD206 expression by $CD45^+F4/80^+CD11b^+$ cells. The subsets of both M1-like ($CD45^+F4/80^+CD11b^+MHCII^{hi}CD206^{low}$) and M2-like ($CD45^+F4/80^+CD11b^+MHCII^{low}CD206^{hi}$) macrophages were much more abundant in dystrophic mice in comparison to WT but the lack of transcriptionally active Nrf2 did not change further their percentage (Fig. 5 H, I, J).

Next, we have studied the population of NK cells and various populations of lymphocytes. The percentage of NK cells ($CD45^+SSC^{low}CD3^-NK1.1^+$) (Fig. 6 A, C), lymphocytes T ($CD45^+SSC^{low}CD3^+$) (Fig. 6 B, C), T helper (T_h; $CD45^+SSC^{low}CD3^+CD8^-CD4^+$) (Fig. 6 D, F), and T cytotoxic (T_c; $CD45^+SSC^{low}CD3^+CD8^+CD4^-$) (Fig. 6 E, F) were the same among four genotypes. Interestingly, despite the lack of differences in the percentage of T regulatory (T_{reg}; $CD45^+SSC^{low}CD3^+CD8^-CD4^+FoxP3^+CD25^+$) cells between dystrophic mice and their healthy counterparts, their level was elevated in $Nrf2^{tKO}$*mdx* compared to *mdx* (Fig. 6 G, H).

The role of Nrf2 transcriptional deficiency on muscle fibrosis

We have found that mRNAs encoding *Tgfb1* and collagen type I alpha 1 (*Col1a1*) were upregulated in *mdx* vs. WT animals and were further elevated in *mdx* mice lacking additionally transcriptionally active Nrf2 (Fig. 7 A, B), suggesting that the transcriptional deficiency of Nrf2 could enhance fibrosis. To confirm those results a histological analysis of collagen deposition based on Masson's trichrome staining was performed. Accordingly, endomysial collagen content was significantly elevated in dystrophic mice in

comparison to WT animals. However, it was not further exacerbated in *mdx* mice lacking transcriptionally active Nrf2 (Fig. 7 C, D).

A decrease in the expression of angiogenic mediators in *mdx* mice is not affected by the lack of transcriptionally active Nrf2

Dysregulation of angiogenesis may greatly contribute to DMD progression (29). Moreover, Nrf2 was shown to regulate neovascularization and exert a pivotal role in angiogenic signal transduction and angiogenic potential of endothelial cells and bone marrow-derived proangiogenic cells (30). Therefore, we aimed to investigate the angiogenic signaling in our model. Firstly, we have checked the mRNA and protein level of the major proangiogenic factor, VEGF, in GM in mice of all genotypes. The mRNA expression was diminished in *mdx* mice but no further changes were observed in double knockouts (Fig. 8 A). Concomitantly, the level of VEGF protein was potently down-regulated in dystrophic gastrocnemius muscle, however, the lack of transcriptionally active Nrf2 did affect this production neither in healthy and dystrophic mice (Fig. 8 B). A similar trend of changes was found when the expression of *Kdr*, receptor for VEGF were evaluated (Fig. 8 C).

Nrf2 transcriptional deficiency does not affect the number and proliferation of muscle SCs but it may influence muscle regeneration

To elucidate whether Nrf2 affects SCs functions, we analysed the number and proliferation of SCs isolated from skeletal muscles of four genotypes: WT, $Nrf2^{tKO}$, *mdx*, $Nrf2^{tKO}$*mdx*. Flow cytometry analysis of SCs ($CD45^-CD31^-Sca1^-\alpha7integrin^+$) percentage among nucleated cells revealed a considerable decrease in dystrophin-deficient mice in comparison to WT counterparts, but it was not further changed by Nrf2 transcriptional deficiency (Fig. 9 A, B). Accordingly, the percentage of quiescent SCs ($CD45^-CD31^-Sca1^-\alpha7integrin^+CD34^+$) was decreased in *mdx* and $Nrf2^{tKO}$*mdx*, but it was not additionally affected by the lack of transcriptionally active Nrf2 (Fig. 9 C). Whereas, the percentage of activated SCs ($CD45^-CD31^-Sca1^-\alpha7integrin^+CD34^-$) did not differ between four genotypes (Fig. 9 D).

Moreover, we have checked the proliferation of $CD34^+$ and $CD34^-$ SCs by cytofluorimetric analysis of cells in S+G2M phase. We have noticed a significant enhancement in the proliferation of both, SCs $CD34^+$ and $CD34^-$ in dystrophic muscles compared to normal mice, but additional influence of Nrf2 transcriptional deficiency was not observed (Fig. 9 E, F).

Importantly, the percentage of SCs analysed among all nucleated cells by flow cytometry can be misleading due to the excessive inflammation in the muscles of *mdx* animals. Therefore, we have additionally analysed SCs number based on IHF staining by counting the ratio of Pax7-positive nuclei to myofibers. According to performed staining, the number of $Pax7^+$ cells was increased in *mdx* mice in comparison to healthy ones (Fig. 9 G, H). However, none of the methods showed the additional effect of the lack of transcriptionally active Nrf2 on SCs number.

Although there is no effect of Nrf2 on the number and proliferation of SCs, we have shown that the regeneration process is affected in the course of chronic injury in dystrophic mice, and what is more – it is additionally altered by the Nrf2 status. Dystrophic mice showed higher expression of myogenic regulatory factors such as myogenic differentiation 1 (*Myod1*) and myogenin (*Myog*) than their healthy counterparts and the expression of those factors was further enhanced by Nrf2 transcriptional deficiency (Fig. 10 A, B).

Additionally, we have checked the mRNA level of muscle-specific microRNAs which also contribute to the process of muscle regeneration (31). Expression of miR-206 was elevated in *mdx* mice in comparison to age-matched WT animals whereas miR-1 and miR-133a/b showed the opposite pattern. However, none of them were affected by Nrf2 transcriptional deficiency (Fig. 10 C-E).

Finally, the number of myofibers expressing the marker of regeneration – eMyHC was diminished in *mdx* mice lacking additionally transcriptionally active Nrf2 in comparison to *mdx* counterparts (Fig. 10 F, G). However, histological analysis of centrally nucleated fibers did not show differences between *mdx* and Nrf2^{tKO}*mdx* animals (Fig. 10 H, I).

Discussion

DMD is still incurable disease and pharmacological treatment with corticosteroids, anti-inflammatory agents, is still the gold standard of care of DMD patients (39). Despite having a beneficial effect on muscle function, these drugs cause many side effects such as delayed puberty and growth, weight gain, adrenal insufficiency, and behavioral disorders (34). Therefore, identifying new targets for anti-inflammatory treatment may contribute to the development of novel therapeutic strategies. Taking into consideration the pleiotropic activity of Nrf2, which drives the expression of anti-inflammatory, anti-oxidant, and cytoprotective genes, we aimed to investigate its role in the acute muscle injury induced by CTX injection and in the progression of DMD using the *mdx* mouse model. In our study we found that the absence of transcriptionally active Nrf2 may be associated with increased muscle degeneration in acute muscle injury, however, it does not significantly affect the pathophysiological hallmarks of DMD progression. Thus, the lack of transcriptionally active Nrf2 does not affect the condition of dystrophic muscles.

Due to the disruption of DGC complex and increased membrane permeability in DMD (35), serum proteins such as IgG and IgM, which are typically found only in circulation, are accumulated in damaged, necrotic myofibers (36). Therefore, we used them as a marker of membrane stability and muscle degeneration. We have shown that the number of necrotic fibers does not differ between *mdx* and Nrf2^{tKO}*mdx* mice. Moreover, although we have found the higher levels of CK and LDH in the serum of dystrophic mice in comparison to their healthy counterparts, their level was not further elevated in dystrophic mice lacking transcriptionally active Nrf2. We have also performed such analysis after a single CTX injury, a model where the kinetics of degeneration and inflammation processes is more stable than during DMD development. Although a similar experimental model was previously utilized by Shelar et al. (37), the

degeneration has not been checked. In our hand, Nrf2 transcriptional deficiency was associated with the aggravation of LDH activity in plasma and enhanced degeneration, evidenced by semi-quantitative analysis of H&E staining. On the other hand, other markers of degeneration and inflammation: percentage of necrotic fibers, the activity of CK, level of MCP-1*, Hmox1*, *Il1b*, and *Il6* remain unchanged indicating that the presence of Nrf2 is not sufficient to protect muscle against CTX injury. Taken together, we have shown that muscle degeneration in our models is not significantly affected by transcriptional deficiency of Nrf2. Concomitantly, lack of transcriptionally active Nrf2 does not affect dystrophic muscle strength, as demonstrated by a similar exercise capacity of *mdx* and Nrf2^{tKO}*mdx* obtained during a treadmill test.

Inflammation is one of the most prominent features of dystrophic muscles. In our studies, contrary to the expectations, inflammation was not exacerbated in dystrophic muscles lacking Nrf2. Histological results showed similar inflammatory cells infiltration of GM of dystrophic mice and mice additionally lacking transcriptional activity of Nrf2. Furthermore, cytometric analysis of macrophages, their subpopulations – M1-like and M2-like macrophages as well as monocytes and NK cells, did not demonstrate any changes in cell number between *mdx* and Nrf2^{tKO}*mdx* animals. Despite the fact T_h and T_c lymphocytes contribute to the pathogenesis of DMD (6) and their functions may be regulated by Nrf2 (38), their quantity was changed neither by dystrophin nor Nrf2 deficiency. Although T_{reg} lymphocytes, a subpopulation of T cells, were shown to be elevated in dystrophic muscles of DMD patients and their depletion aggravate inflammation in *mdx* mice (7), we did not observe T_{reg} increase in our *mdx* animals. Nevertheless, T_{reg} number was increased in Nrf2^{tKO}*mdx* in comparison to *mdx*. Interestingly, this finding is consistent with the recent study showing Nrf2 as negative regulator of T_{reg} cells (39). Importantly, our data are in a line with work by Takemoto et al. in which Nrf2 transcriptional deficiency has not exacerbated inflammation in the diaphragm of *mdx* mice (40), the muscle which is the most severely affected in DMD.

Petrillo et al. demonstrated increased expression of Nrf2 and its target, HO-1, in muscle biopsies from DMD patients (16). In our model, we observed an elevated level of HO-1 in the CTX-injured muscles at day 1 after injection, as well as in the dystrophic mice, consistent with our previous results (10,11). However, contrary to expectations, the effect of Nrf2 deficiency on the level of this important inflammatory mediator has been noticed neither in Nrf2^{tKO}*mdx* nor in Nrf2^{tKO} following CTX injury indicating that HO-1 may be regulated independently of Nrf2. Those data might suggest the involvement of compensatory mechanisms protecting from both, acute and chronic muscle injury, in the absence of Nrf2.

Concomitantly, we have revealed that Nrf2 plays a dispensable role in endomysial fibrosis in dystrophic muscles, the process of accumulation of connective tissue, which is the characteristic attribute of DMD pathology (4) and is associated with poor outcome (41). Several studies have already outlined that the level of transforming growth factor (TGFβ-1), the main mediator of fibrosis, is increased in muscles and plasma of DMD patients (42). Similarly, collagen, the main component of fibrotic scar, has been elevated in muscles of murine (43) and canine (44) models of DMD, as well as in dystrophic patients (45). In our model, we have observed elevated mRNA level of *Tgfb1* and *Col1a1* not only in *mdx* mice but even at a higher degree in dystrophic mice additionally lacking transcriptionally active Nrf2, what is consistent with

previous studies showing that Nrf2 acts as a protective agent against fibrosis in different tissues – lungs (46), pancreas (47), and kidney (48). Although the lack of transcription activity of Nrf2 in dystrophic mice affected transcription of fibrotic genes like *Tgfb* and *Col1a1*, it was not reflected in the fibrotic phenotype. Collagen deposition based on Masson's trichome staining were comparable between *mdx* and Nrf2^{tKO}*mdx* animals. The observed differences may be caused by the fact, that the mRNA level reflects a particular time-point, whereas collagen deposition showed changes arising during disease progression. These results were confirmed by no differences in body weight and GM mass between *mdx* and Nrf2^{tKO}*mdx* animals, indicating a similar amount of connective and adipose tissue in both genotypes. Of note, body weight and muscle mass were notably increased in *mdx* animals in comparison to WT mice, the effect caused mostly by the accumulation of fat and connective tissue, resulting in so-called pseudohypertrophy (49).

Despite enhanced fibrosis, the down-regulation of angiogenesis may contribute to DMD progression (reviewed in (29)). In our previous study, we have revealed a decreased level of pro-angiogenic VEGF in dystrophic mice (23) and a similar effect was confirmed in the present research. Moreover, the expression of the VEGF receptor, *Kdr,* was diminished in *mdx* animals. Although Nrf2 was shown to regulate angiogenesis (30), in our conditions it did not affect the expression of the abovementioned angiogenic mediators.

One of the greatest features of skeletal muscle is their remarkable ability to regenerate, a process that is responsible for tissue repair after damage by injury (50). Effective muscle regeneration is achieved by SCs (51). In DMD however repeated cycles of muscle damage and regeneration disturbed balance between self-renewal and differentiation, lead to premature depletion of the SCs pool (52). Firstly, we have shown that the number and proliferation of SCs are similar in the skeletal muscle of wild type and Nrf2^{tKO} mice, what is consistent with the previous studies confirming that Nrf2 transcriptional deficiency does not affect healthy skeletal muscle (40,53). When dystrophic animals were examined, a striking decline of SCs relative number in comparison to WT was revealed by the cytometric analysis. However, since dystrophic skeletal muscles are infiltrated by a large number of inflammatory cells, it may significantly affect those results, decreasing the percentage of non-immune cell types. The absolute number of SCs, based on the Pax7-positive myofibers was notably increased in dystrophic animals. Concomitantly, we have noticed a significant enhancement in SCs proliferation in dystrophic muscles compared to healthy ones, which is in line with the previous studies performed on *mdx* mice (54). Nevertheless, regardless of the method used, the number, as well as the proliferation of SCs, was not altered by Nrf2 transcriptional deficiency.

As muscle regeneration is controlled by myogenic regulatory factors (MRFs) such as MyoD and myogenin, we have checked their mRNA expression in our model showing that expression of *Myod1* and *Myog* was significantly increased in *mdx* mice. Moreover, its level was further upregulated by Nrf2 transcriptional deficiency. Apart from MRFs, skeletal muscle myogenesis may be regulated by a group of miRNAs (miR-1, miR133a/b, miR-206), called myomiRs, which expression is characteristic for skeletal muscle and cardiomyocytes (31). We have shown the reduced expression of miR-1 and miR-133a/b and

upregulated of miR-206 in *mdx* mice. It is consistent with literature showing elevated level of miR-206 in dystrophic muscles due to its expression in differentiating satellite cells (55). Nevertheless, expression of myomiRs was not further changed by lack of transcriptionally active Nrf2.

Newly formed myofibers are characterized by the expression of unique myosin isoforms such as eMyHC. The number of eMyHC-positive myofibers was lower in *mdx* mice additionally lacking transcriptional activity of Nrf2 in comparison to *mdx*, whereas the number of centrally nucleated myofibers was similar between those two genotypes. Developmental myosins such as eMyHC may serve as a marker of current (56), while centrally nucleated myofibers of cumulative muscle regeneration (57), which may explain this difference. Because there are many repeated cycles of muscle damage and regeneration in DMD, it is difficult to conclude how Nrf2 affects this process based on transiently expressed eMyHC (56). Therefore, we also checked muscle regeneration after acute muscle injury induced by CTX injection, methods that allow studying muscle regeneration in more controlled and reproducible conditions (58). We have shown that expression of *Myh3*, gene encoding eMyHC, and number of eMyHC- positive myofibers were comparable between WT and $Nrf2^{tKO}$ mice following CTX injection indicated that muscle regeneration is not affected by the lack of transcriptionally active Nrf2. This finding is consistent with previous studies where similar level of regeneration in transcriptionally deficient Nrf2 and control mice was demonstrated (40). Whereas, Shelar et al presented delayed regeneration in Nrf2-deficnet mice, however, they used much older mice – 6-8-months-old (37).

Overall, our results did not show the prominent effects of Nrf2 deficiency both in acute and in chronic muscle injury. The other situation may happen with Nrf2 induction or overexpression. Sun et al. have shown that dystrophic phenotype may be markedly alleviated in *mdx* mice by treatment with sulforaphane, SFN (17,19), an isothiocyanate that activates Nrf2 by modifying Keap1 cysteines (59). The oral administration of SFN to *mdx* mice for 4-8 months resulted in improved muscle strength, increased muscle weight, decreased LDH and CK activities in plasma as well as oxidative stress and inflammation in dystrophic muscles (17,19). Moreover, several studies have outlined that some features of DMD might be improved by other antioxidant compounds like resveratrol (60,61) or curcumin (62), but their effect was not as strong as SFN (17,19). However, it is important to remember that such compounds might work not necessarily through activation of Nrf2, but they may also involve other mechanisms (63–65), and in the above studies the involvement of the Nrf2 pathway was not investigated.

In conclusion, our study shows that the lack of transcriptionally active Nrf2 does not contribute potently to acute and chronic myodamage. However, further studies, e.g. performed in older animals may be of importance to fully understand the potential role of Nrf2 in dystrophy progression.

Conclusion

Lack of transcriptionally active Nrf2 is associated with slightly increased muscle degeneration in acute muscle injury caused by CTX injection. Moreover, during chronic disorder – DMD, transcriptional deficiency of Nrf2 affects some markers of muscle regeneration and increases expression of *Tgfb* and

Col1a1. Nevertheless, Nrf2 ablation does not significantly aggravate the most deleterious pathological events such as degeneration, inflammation, decreased angiogenesis and fibrosis scar formation as well as the number and proliferation of SCs during the progression of DMD in *mdx* mice.

Abbreviations

ARE – antioxidant response element

BSA – bovine serum albumin

CK – creatine kinase

Col1a1 – collagen type I alpha 1

CTX – cardiotoxin

DGC – dystrophin-glycoprotein complex

DMD – Duchenne muscular dystrophy

Eef2 – eukaryotic elongation factor 2

eMyHC – embryonic myosin heavy chain

GM – gastrocnemius muscle

H&E - hematoxylin and eosin

Hmox1 – gene encoding HO-1

HO-1 – heme oxygenase-1

IHF – immunohistofluorescent

Il1b – Interleukin 1 beta

Il6 – Interleukin 6

Keap1 – Kelch-like ECH-associating protein 1

Kdr – receptor for VEGF (VEGF-R2)

LDH – lactate dehydrogenase

MCP-1 – monocyte chemoattractant protein 1

MRFs - muscle regulatory factors

M.O.M – mouse on mouse

Myh3 – myosin heavy chain 3

Myog – myogenin

NK – natural killer

Nrf2 – nuclear factor erythroid 2-related factor 2

OCT – optimal cutting temperature compound

Pax7 – paired box 7

PBS – phosphate-buffered saline

PCR – polymerase chain reaction

qPCR – quantitative PCR

ROS – reactive oxygen species

SCs – satellite cells

SEM – standard error of the mean

T_c – lymphocytes T cytotoxic

TGF-b - transforming growth factor-β

T_h – lymphocytes T helper

Tie1 - tyrosine kinase with immunoglobulin-like and EGF-like domains 1

T_{reg} – lymphocytes T regulatory

VEGF – vascular endothelial growth factor

WT – wild type

Declarations

Acknowledgments

We are grateful to the staff of the animal facility of the Faculty of Biochemistry, Biophysics and Biotechnology for help in animal breeding. Anna Gese and Ryszard Czypicki are acknowledged for technical help with cardiotoxin experiment. We would like to thank the administrative staff of the

Department of Medical Biotechnology for their assistance; Prof. Frederic Relaix and Dr. Audrey Der Vartanian (INSERM, France) for providing the protocol for Pax7 staining.

Authors' contributions

IBB performed the research, designed the research, acquired and analysed the data, wrote the manuscript; MK performed the research, designed the research, acquired and analysed the data; AŁ performed the research, interpreted the data and contributed to manuscript writing; JD designed the research, supervised the study and contributed to manuscript writing. All authors read and approved the final manuscript.

Ethics approval and consent to participate

All animal procedures and experiments were performed in accordance with national and European legislation, after approval by the 1st and 2nd Institutional Animal Care and Use Committee (IACUC) in Kraków, Poland (approval number: 66/2013 and 199/2018).

Consent for publication

Not applicable.

Availability of data and materials

The datasets used and/or analysed during the current study are available from the corresponding author on reasonable request.

Competing interests

The authors declare that they have no competing interests.

Funding

This work was supported by the National Science Centre: grants MAESTRO – 2012/06/A/NZ1/00004 (JD), OPUS – 2016/21/B/NZ1/00293 (AŁ) and the Grant for Young Researchers – BMN 7/2017 (IBB)

funded by the Faculty of Biochemistry, Biophysics and Biotechnology of the Jagiellonian University in Kraków.

References

1. Emery AE. The muscular dystrophies. The Lancet. 2002 Feb;359(9307):687–95.
2. Mendell JR, Rodino-Klapac LR, Sahenk Z, Roush K, Bird L, Lowes LP, et al. Eteplirsen for the treatment of Duchenne muscular dystrophy: Eteplirsen for DMD. Ann Neurol. 2013 Nov;74(5):637–47.
3. Matsumura K, Campbell KP. Dystrophin-glycoprotein complex: Its role in the molecular pathogenesis of muscular dystrophies. Muscle Nerve. 1994 Jan;17(1):2–15.
4. Rosenberg AS, Puig M, Nagaraju K, Hoffman EP, Villalta SA, Rao VA, et al. Immune-mediated pathology in Duchenne muscular dystrophy. Sci Transl Med. 2015 Aug 5;7(299):299rv4-299rv4.
5. Tidball JG. Mechanisms of Muscle Injury, Repair, and Regeneration. In: Terjung R, editor. Comprehensive Physiology [Internet]. Hoboken, NJ, USA: John Wiley & Sons, Inc.; 2011 [cited 2020 Mar 26]. p. c100092. Available from: http://doi.wiley.com/10.1002/cphy.c100092
6. Spencer MJ, Montecino-Rodriguez E, Dorshkind K, Tidball JG. Helper (CD4+) and Cytotoxic (CD8+) T Cells Promote the Pathology of Dystrophin-Deficient Muscle. Clinical Immunology. 2001 Feb;98(2):235–43.
7. Villalta SA, Rosenthal W, Martinez L, Kaur A, Sparwasser T, Tidball JG, et al. Regulatory T cells suppress muscle inflammation and injury in muscular dystrophy. Science Translational Medicine. 2014 Oct 15;6(258):258ra142-258ra142.
8. Tidball JG, Wehling-Henricks M. The role of free radicals in the pathophysiology of muscular dystrophy. Journal of Applied Physiology. 2007 Apr;102(4):1677–86.
9. Rando TA, Disatnik M-H, Yu Y, Franco A. Muscle cells from mdx mice have an increased susceptibility to oxidative stress. Neuromuscular Disorders. 1998 Feb;8(1):14–21.
10. Pietraszek-Gremplewicz K, Kozakowska M, Bronisz-Budzynska I, Ciesla M, Mucha O, Podkalicka P, et al. Heme Oxygenase-1 Influences Satellite Cells and Progression of Duchenne Muscular Dystrophy in Mice. Antioxidants & Redox Signaling. 2018 Jul 10;29(2):128–48.
11. Kozakowska M, Pietraszek-Gremplewicz K, Ciesla M, Seczynska M, Bronisz-Budzynska I, Podkalicka P, et al. Lack of Heme Oxygenase-1 Induces Inflammatory Reaction and Proliferation of Muscle Satellite Cells after Cardiotoxin-Induced Skeletal Muscle Injury. The American Journal of Pathology. 2018 Feb;188(2):491–506.
12. Alam J, Stewart D, Touchard C, Boinapally S, Choi AMK, Cook JL. Nrf2, a Cap'n'Collar Transcription Factor, Regulates Induction of the Heme Oxygenase-1 Gene. J Biol Chem. 1999 Sep 10;274(37):26071–8.
13. Sykiotis GP, Bohmann D. Stress-Activated Cap'n'collar Transcription Factors in Aging and Human Disease. Science Signaling. 2010 Mar 9;3(112):re3–re3.

14. Ahn B, Pharaoh G, Premkumar P, Huseman K, Ranjit R, Kinter M, et al. Nrf2 deficiency exacerbates age-related contractile dysfunction and loss of skeletal muscle mass. Redox Biol. 2018;17:47–58.
15. Done AJ, Traustadóttir T. Nrf2 mediates redox adaptations to exercise. Redox Biol. 2016;10:191–9.
16. Petrillo S, Pelosi L, Piemonte F, Travaglini L, Forcina L, Catteruccia M, et al. Oxidative stress in Duchenne muscular dystrophy: focus on the NRF2 redox pathway. Hum Mol Genet. 2017 15;26(14):2781–90.
17. Sun C-C, Li S-J, Yang C-L, Xue R-L, Xi Y-Y, Wang L, et al. Sulforaphane Attenuates Muscle Inflammation in Dystrophin-deficient *mdx* Mice via NF-E2-related Factor 2 (Nrf2)-mediated Inhibition of NF-κB Signaling Pathway. J Biol Chem. 2015 Jul 17;290(29):17784–95.
18. Sun C, Li S, Li D. Sulforaphane mitigates muscle fibrosis in *mdx* mice via Nrf2-mediated inhibition of TGF-β/Smad signaling. Journal of Applied Physiology. 2016 Feb 15;120(4):377–90.
19. Sun C, Yang C, Xue R, Li S, Zhang T, Pan L, et al. Sulforaphane alleviates muscular dystrophy in *mdx* mice by activation of Nrf2. Journal of Applied Physiology. 2015 Jan 15;118(2):224–37.
20. Itoh K, Chiba T, Takahashi S, Ishii T, Igarashi K, Katoh Y, et al. An Nrf2/small Maf heterodimer mediates the induction of phase II detoxifying enzyme genes through antioxidant response elements. Biochem Biophys Res Commun. 1997 Jul 18;236(2):313–22.
21. Kloska D, Kopacz A, Cysewski D, Aepfelbacher M, Dulak J, Jozkowicz A, et al. Nrf2 Sequesters Keap1 Preventing Podosome Disassembly: A Quintessential Duet Moonlights in Endothelium. Antioxid Redox Signal. 2019 May 10;30(14):1709–30.
22. Innamorato NG, Jazwa A, Rojo AI, García C, Fernández-Ruiz J, Grochot-Przeczek A, et al. Different susceptibility to the Parkinson's toxin MPTP in mice lacking the redox master regulator Nrf2 or its target gene heme oxygenase-1. PLoS ONE. 2010 Jul 28;5(7):e11838.
23. Bronisz-Budzyńska I, Chwalenia K, Mucha O, Podkalicka P, Karolina-Bukowska-Strakova, Józkowicz A, et al. miR-146a deficiency does not aggravate muscular dystrophy in mdx mice. Skeletal Muscle. 2019 Dec;9(1):22.
24. Giordano C, Mojumdar K, Liang F, Lemaire C, Li T, Richardson J, et al. Toll-like receptor 4 ablation in mdx mice reveals innate immunity as a therapeutic target in Duchenne muscular dystrophy. Human Molecular Genetics. 2015 Apr 15;24(8):2147–62.
25. Liu N, Williams AH, Maxeiner JM, Bezprozvannaya S, Shelton JM, Richardson JA, et al. microRNA-206 promotes skeletal muscle regeneration and delays progression of Duchenne muscular dystrophy in mice. J Clin Invest. 2012 Jun 1;122(6):2054–65.
26. Nitahara-Kasahara Y, Hayashita-Kinoh H, Chiyo T, Nishiyama A, Okada H, Takeda S, et al. Dystrophic mdx mice develop severe cardiac and respiratory dysfunction following genetic ablation of the anti-inflammatory cytokine IL-10. Human Molecular Genetics. 2014 Aug 1;23(15):3990–4000.
27. Vomund S, Schäfer A, Parnham M, Brüne B, von Knethen A. Nrf2, the Master Regulator of Anti-Oxidative Responses. IJMS. 2017 Dec 20;18(12):2772.
28. Kobayashi EH, Suzuki T, Funayama R, Nagashima T, Hayashi M, Sekine H, et al. Nrf2 suppresses macrophage inflammatory response by blocking proinflammatory cytokine transcription. Nat

Commun. 2016 Sep;7(1):11624.

29. Podkalicka P, Mucha O, Dulak J, Loboda A. Targeting angiogenesis in Duchenne muscular dystrophy. Cell Mol Life Sci. 2019 Apr;76(8):1507–28.
30. Florczyk U, Jazwa A, Maleszewska M, Mendel M, Szade K, Kozakowska M, et al. Nrf2 regulates angiogenesis: effect on endothelial cells, bone marrow-derived proangiogenic cells and hind limb ischemia. Antioxid Redox Signal. 2014 Apr 10;20(11):1693–708.
31. Chen J-F, Mandel EM, Thomson JM, Wu Q, Callis TE, Hammond SM, et al. The role of microRNA-1 and microRNA-133 in skeletal muscle proliferation and differentiation. Nat Genet. 2006 Feb;38(2):228–33.
32. Falzarano M, Scotton C, Passarelli C, Ferlini A. Duchenne Muscular Dystrophy: From Diagnosis to Therapy. Molecules. 2015 Oct 7;20(10):18168–84.
33. McDonald CM, Henricson EK, Abresch RT, Duong T, Joyce NC, Hu F, et al. Long-term effects of glucocorticoids on function, quality of life, and survival in patients with Duchenne muscular dystrophy: a prospective cohort study. The Lancet. 2018 Feb;391(10119):451–61.
34. Wood CL, Straub V, Guglieri M, Bushby K, Cheetham T. Short stature and pubertal delay in Duchenne muscular dystrophy. Arch Dis Child. 2016 Jan;101(1):101–6.
35. Matsumura K, Tomé FM, Ionasescu V, Ervasti JM, Anderson RD, Romero NB, et al. Deficiency of dystrophin-associated proteins in Duchenne muscular dystrophy patients lacking COOH-terminal domains of dystrophin. J Clin Invest. 1993 Aug 1;92(2):866–71.
36. Straub V, Rafael JA, Chamberlain JS, Campbell KP. Animal Models for Muscular Dystrophy Show Different Patterns of Sarcolemmal Disruption. J Cell Biol. 1997 Oct 20;139(2):375–85.
37. Shelar SB, Narasimhan M, Shanmugam G, Litovsky SH, Gounder SS, Karan G, et al. Disruption of nuclear factor (erythroid-derived-2)–like 2 antioxidant signaling: a mechanism for impaired activation of stem cells and delayed regeneration of skeletal muscle. The FASEB Journal. 2016 May;30(5):1865–79.
38. Tsai JJ, Velardi E, Shono Y, Argyropoulos KV, Holland AM, Smith OM, et al. Nrf2 regulates CD4+ T cell–induced acute graft-versus-host disease in mice. Blood. 2018 Dec 27;132(26):2763–74.
39. Klemm P, Rajendiran A, Fragoulis A, Wruck C, Schippers A, Wagner N, et al. Nrf2 expression driven by Foxp3 specific deletion of Keap1 results in loss of immune tolerance in mice. Eur J Immunol. 2020 Apr;50(4):515–24.
40. Takemoto Y, Inaba S, Zhang L, Tsujikawa K, Uezumi A, Fukada S. Implication of basal lamina dependency in survival of Nrf2-null muscle stem cells via an antioxidative-independent mechanism: TAKEMOTO et al. J Cell Physiol. 2019 Feb;234(2):1689–98.
41. Desguerre I, Mayer M, Leturcq F, Barbet J-P, Gherardi RK, Christov C. Endomysial Fibrosis in Duchenne Muscular Dystrophy: A Marker of Poor Outcome Associated With Macrophage Alternative Activation. J Neuropathol Exp Neurol. 2009 Jul;68(7):762–73.
42. Ishitobi M, Haginoya K, Zhao Y, Ohnuma A, Minato J, Yanagisawa T, et al. Elevated plasma levels of transforming growth factor β1 in patients with muscular dystrophy: NeuroReport. 2000

Dec;11(18):4033–5.

43. Ieronimakis N, Hays A, Prasad A, Janebodin K, Duffield JS, Reyes M. PDGFRα signalling promotes fibrogenic responses in collagen-producing cells in Duchenne muscular dystrophy: PDGFRα signalling promotes fibrosis in Duchenne muscular dystrophy. J Pathol. 2016 Dec;240(4):410–24.
44. Gaiad TP, Araujo KPC, Serrão JC, Miglino MA, Ambrósio CE. Motor Physical Therapy Affects Muscle Collagen Type I and Decreases Gait Speed in Dystrophin-Deficient Dogs. Huard J, editor. PLoS ONE. 2014 Apr 8;9(4):e93500.
45. Pines M, Levi O, Genin O, Lavy A, Angelini C, Allamand V, et al. Elevated Expression of Moesin in Muscular Dystrophies. The American Journal of Pathology. 2017 Mar;187(3):654–64.
46. Cho H-Y, Reddy SPM, Yamamoto M, Kleeberger SR. The transcription factor NRF2 protects against pulmonary fibrosis. The FASEB Journal. 2004 Aug;18(11):1258–60.
47. Kojayan GG, Alizadeh RF, Li S, Ichii H. Reducing Pancreatic Fibrosis Using Antioxidant Therapy Targeting Nrf2 Antioxidant Pathway: A Possible Treatment for Chronic Pancreatitis. Pancreas. 2019;48(10):1259–62.
48. Stachurska A, Ciesla M, Kozakowska M, Wolffram S, Boesch-Saadatmandi C, Rimbach G, et al. Cross-talk between microRNAs, nuclear factor E2-related factor 2, and heme oxygenase-1 in ochratoxin A-induced toxic effects in renal proximal tubular epithelial cells. Mol Nutr Food Res. 2013 Mar;57(3):504–15.
49. Kornegay JN, Childers MK, Bogan DJ, Bogan JR, Nghiem P, Wang J, et al. The paradox of muscle hypertrophy in muscular dystrophy. Phys Med Rehabil Clin N Am. 2012 Feb;23(1):149–72, xii.
50. Sirabella D, De Angelis L, Berghella L. Sources for skeletal muscle repair: from satellite cells to reprogramming. J Cachexia Sarcopenia Muscle. 2013 Jun;4(2):125–36.
51. Relaix F, Zammit PS. Satellite cells are essential for skeletal muscle regeneration: the cell on the edge returns centre stage. Development. 2012 Aug 15;139(16):2845–56.
52. Heslop L, Morgan JE, Partridge TA. Evidence for a myogenic stem cell that is exhausted in dystrophic muscle. J Cell Sci. 2000 Jun;113 (Pt 12):2299–308.
53. Yamaguchi M, Murakami S, Yoneda T, Nakamura M, Zhang L, Uezumi A, et al. Evidence of Notch-Hesr-Nrf2 Axis in Muscle Stem Cells, but Absence of Nrf2 Has No Effect on Their Quiescent and Undifferentiated State. Musaro A, editor. PLoS ONE. 2015 Sep 29;10(9):e0138517.
54. Yablonka-Reuveni Z, Anderson JE. Satellite cells from dystrophic (Mdx) mice display accelerated differentiation in primary cultures and in isolated myofibers. Dev Dyn. 2006 Jan;235(1):203–12.
55. Cacchiarelli D, Martone J, Girardi E, Cesana M, Incitti T, Morlando M, et al. MicroRNAs Involved in Molecular Circuitries Relevant for the Duchenne Muscular Dystrophy Pathogenesis Are Controlled by the Dystrophin/nNOS Pathway. Cell Metabolism. 2010 Oct;12(4):341–51.
56. Schiaffino S, Rossi AC, Smerdu V, Leinwand LA, Reggiani C. Developmental myosins: expression patterns and functional significance. Skeletal Muscle. 2015 Dec;5(1):22.

57. Coulton GR, Morgan JE, Partridge TA, Sloper JC. THE mdx MOUSE SKELETAL MUSCLE MYOPATHY: I. A HISTOLOGICAL, MORPHOMETRIC AND BIOCHEMICAL INVESTIGATION. Neuropathol Appl Neurobiol. 1988 Feb;14(1):53–70.
58. Chargé SBP, Rudnicki MA. Cellular and Molecular Regulation of Muscle Regeneration. Physiological Reviews. 2004 Jan;84(1):209–38.
59. Hu C, Eggler AL, Mesecar AD, van Breemen RB. Modification of Keap1 Cysteine Residues by Sulforaphane. Chem Res Toxicol. 2011 Apr 18;24(4):515–21.
60. Gordon BS, Delgado-Diaz DC, Carson J, Fayad R, Wilson LB, Kostek MC. Resveratrol improves muscle function but not oxidative capacity in young mdx mice. Can J Physiol Pharmacol. 2014 Mar;92(3):243–51.
61. Hori YS, Kuno A, Hosoda R, Tanno M, Miura T, Shimamoto K, et al. Resveratrol Ameliorates Muscular Pathology in the Dystrophic *mdx* Mouse, a Model for Duchenne Muscular Dystrophy. J Pharmacol Exp Ther. 2011 Sep;338(3):784–94.
62. Pan Y, Chen C, Shen Y, Zhu C-H, Wang G, Wang X-C, et al. Curcumin alleviates dystrophic muscle pathology in mdx mice. Mol Cells. 2008 Jun 30;25(4):531–7.
63. Berman AY, Motechin RA, Wiesenfeld MY, Holz MK. The therapeutic potential of resveratrol: a review of clinical trials. npj Precision Onc. 2017 Dec;1(1):35.
64. Liang J, Hänsch GM, Hübner K, Samstag Y. Sulforaphane as anticancer agent: A double-edged sword? Tricky balance between effects on tumor cells and immune cells. Advances in Biological Regulation. 2019 Jan;71:79–87.
65. Durham A, Jazrawi E, Rhodes JA, Williams C, Kilty I, Barnes P, et al. The anti-inflammatory effects of sulforaphane are not mediated by the Nrf2 pathway. European Respiratory Journal [Internet]. 2014 Sep 1 [cited 2019 Nov 17];44(Suppl 58). Available from: https://erj.ersjournals.com/content/44/Suppl_58/P3332

Figures

Fig. 1.

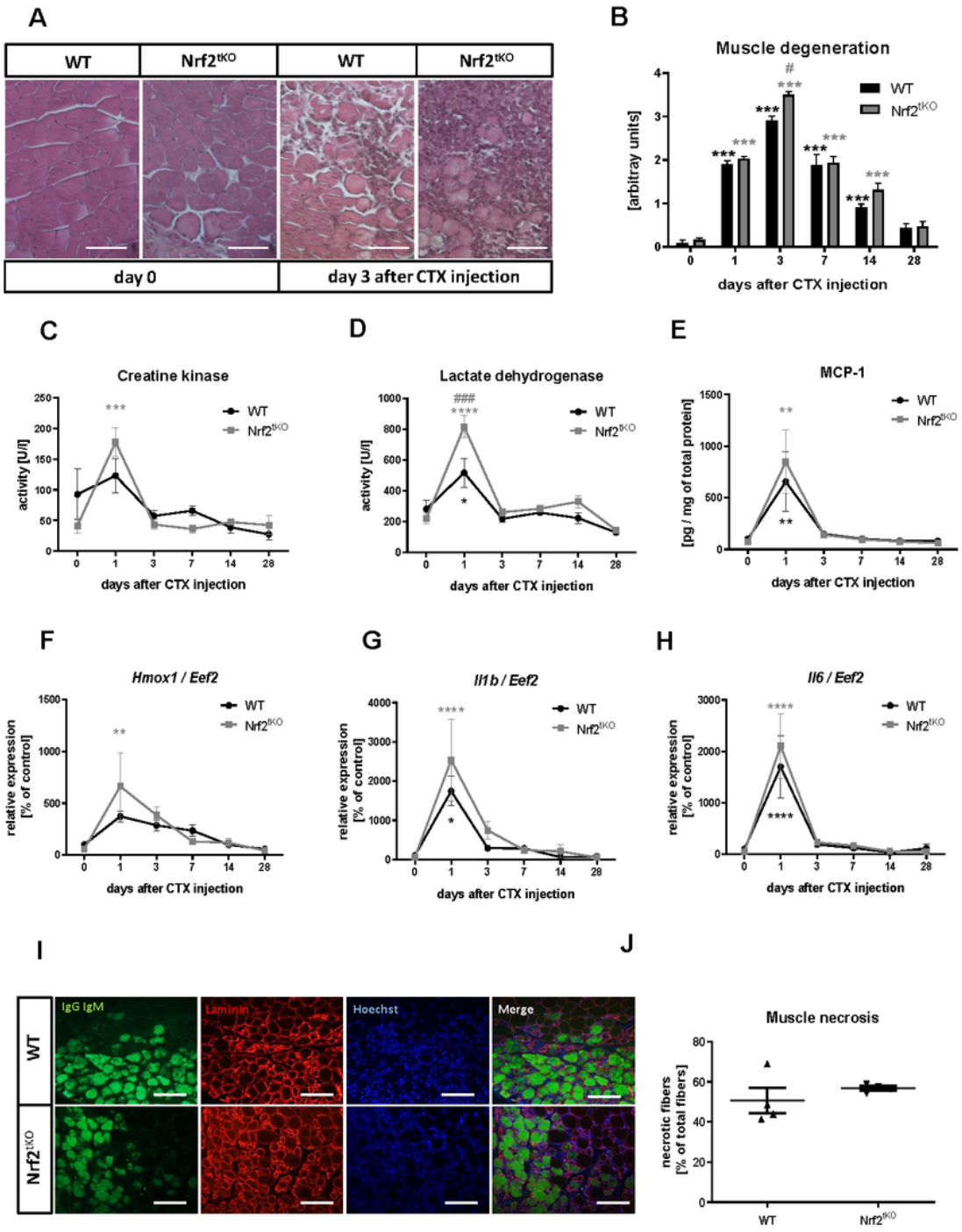

Figure 1

CTX-induced injury in GM of WT and Nrf2tKO animals. (A) Representative photos and (B) semi-quantitative assessment of GM degeneration based on H&E staining; n=4-6. (C) The activity of LDH and (D) CK in plasma; activity assay; n=4-5. (E) MCP-1 protein level in GM, LuminexTM; n=4-5. (F) Hmox1, (G) Il1b, (H) Il6 level in GM; qRT-PCR; n=4-6. (I) Representative photos of microscopic assessment of myofiber necrosis in GM and (J) quantification of the staining; n=4. The data are presented as mean +/- SEM;

*p≤0.05; **p≤0.01; ***p≤0.001; ****p≤0.0001 vs day 0; #p≤0.05; ### p≤0.001 vs WT. The scale bars represent 100 µm.

Fig. 2.

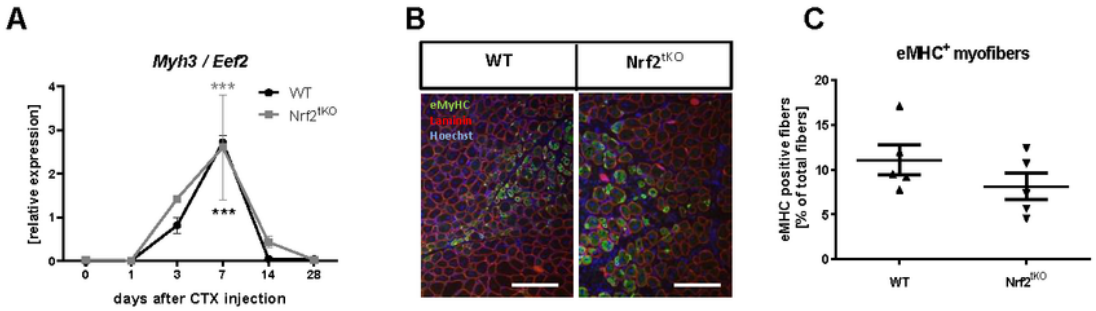

Figure 2

Muscle regeneration in GM of WT and Nrf2tKO animals after CTX-induced injury. (A) Myh3 level in GM; qRT-PCR; n= 4-6. (B) Representative photos of immunofluorescent staining for eMyHC and (C)

quantification of the percentage of eMyHC positive myofibers; n=5. The data are presented as mean +/- SEM; ***p≤0.001 vs day 0. The scale bars represent 100 µm.

Fig. 3.

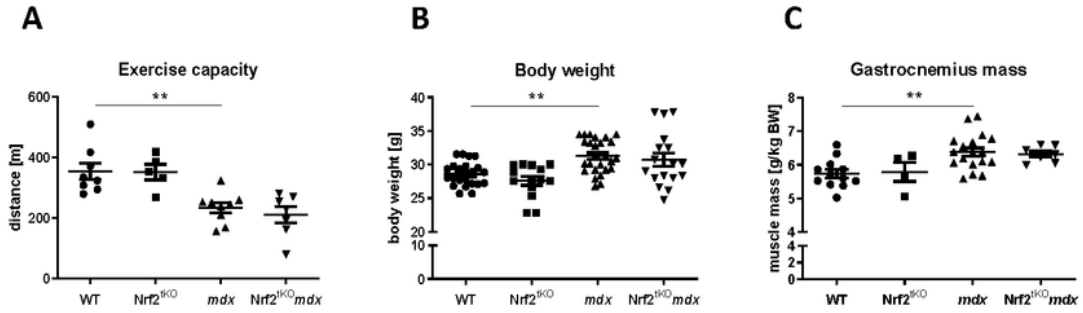

Figure 3

General phenotype of WT, Nrf2tKO, mdx and Nrf2tKOmdx mice. (A) Muscle performance; downhill running treadmill test; n=5-9. (B) Body weight of mice; n=14-26; (C) Gastrocnemius muscle mass; n=4-18. The data are presented as mean +/- SEM; ** p≤0.01.

Fig. 4.

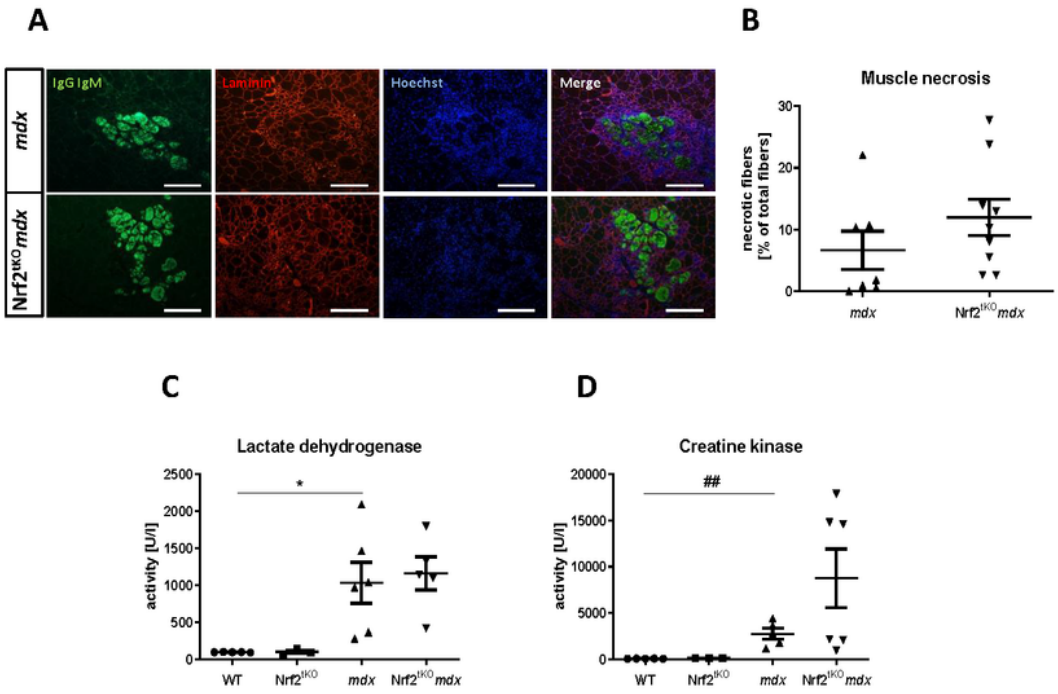

Figure 4

Muscle degeneration of WT, Nrf2tKO, mdx and Nrf2tKOmdx mice. (A) Microscopic assessment of myofiber necrosis in GM using immunofluorescent staining of IgM and IgG (green) binding and (B) its calculation; n=7-9. (C) The activity of LDH and (D) CK in plasma; activity assay; n=3-6. The data are presented as mean +/- SEM; *p≤0.05, one-way ANOVA with Tukey's post-hoc test; ## p≤0.01 Student's t-test. The scale bars represent 100 μm.

Fig. 5.

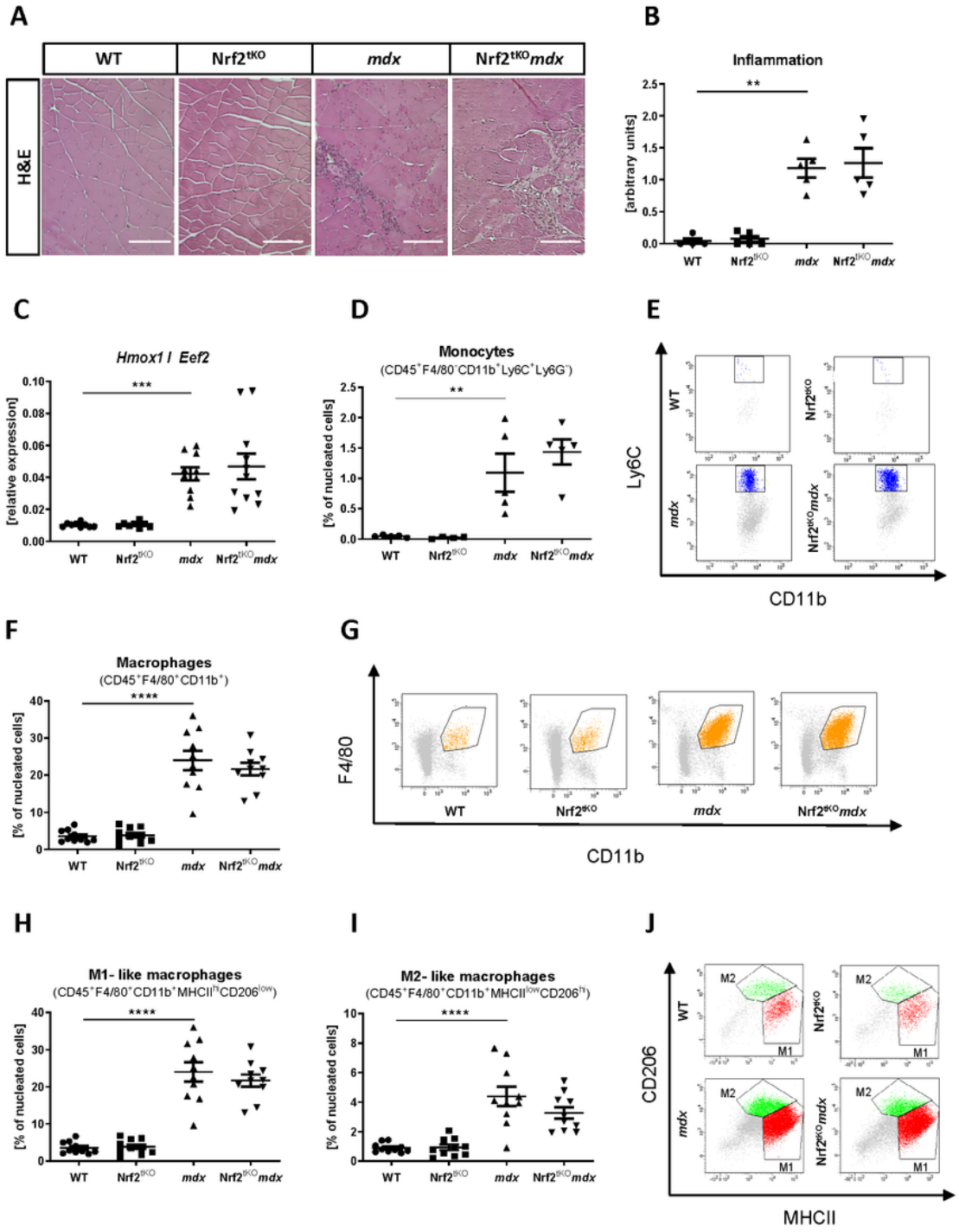

Figure 5

Infiltration of WT, Nrf2tKO, mdx and Nrf2tKOmdx hind limb muscle with leukocytes, monocytes, and macrophages. (A) Representative photos and (B) semi-quantitative analysis of inflammation in GM based on H&E staining; n=4-6. (C) Hmox1 level in GM; qRT-PCR; n=8-11. (D) Percentage of monocytes (CD45+F4/80-CD11b+Ly6C+Ly6G-); flow cytometry; n=5; (E) gating strategy. (F) Percentage of CD45+F4/80+CD11b+ macrophages; flow cytometry; n=10; (G) gating strategy. (H) Percentage of M1-like

macrophages (CD45+F4/80+CD11b+MHCIIhiCD206lo) and (I) M2-like macrophages (CD45+F4/80+CD11b+MHCIIloCD206hi); flow cytometry; n=10; (J) gating strategy. The data are presented as mean +/- SEM; ** p≤0.01; ***p≤0.001; ****p≤0.0001. The scale bars represent 100 µm.

Fig. 6.

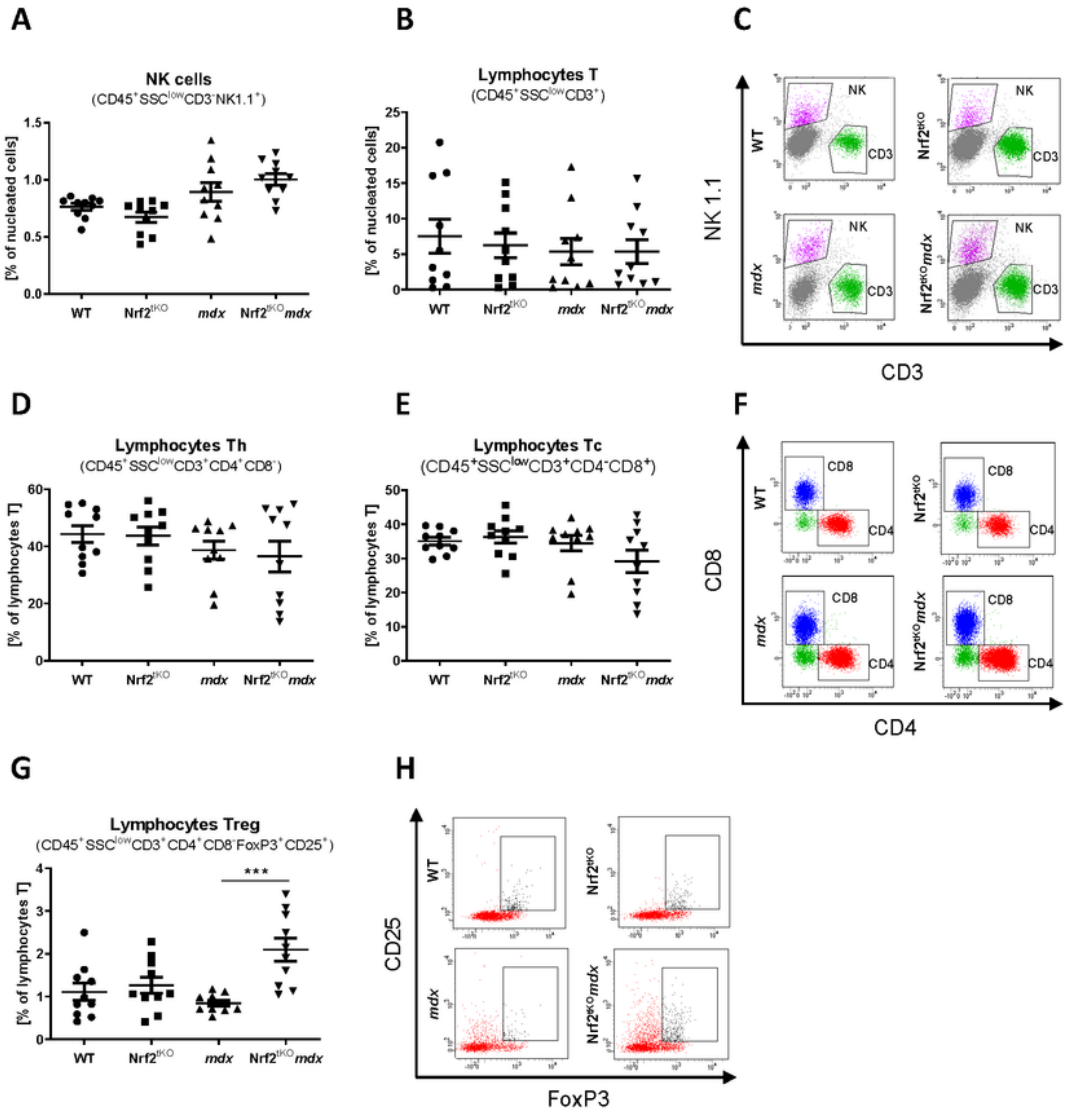

Figure 6

Infiltration of WT, Nrf2tKO, mdx and Nrf2tKOmdx hind limb muscle with NK cells and lymphocytes. (A) Percentage of NK cells (CD45+SSClowCD3-NK1.1+) and (B) lymphocytes T (CD45+SSClowCD3+); flow

cytometry; (C) gating strategy. (D) Percentage of lymphocytes Th (CD45+SSClowCD3+CD4+CD8-) and (E) Tc (CD45+SSClowCD3+CD4-CD8+); flow cytometry; (F) gating strategy. (G) Percentage of lymphocytes Treg (CD45+SSClowCD3+CD4+CD8-FoxP3+CD25+); flow cy

Fig. 7.

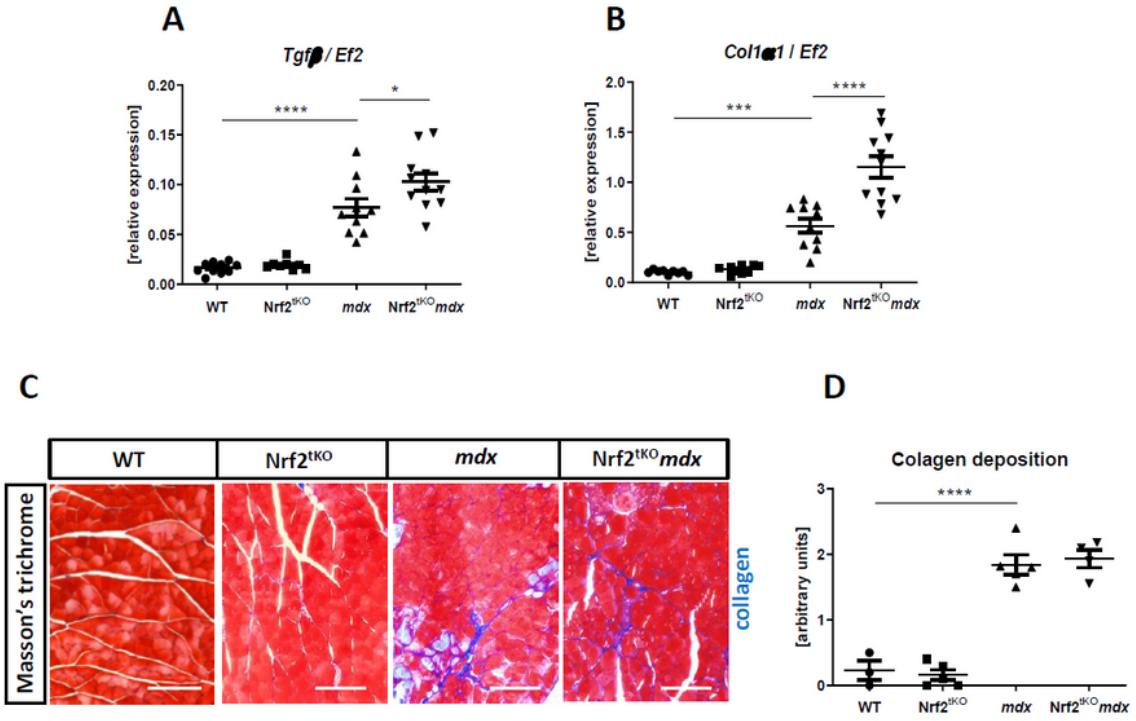

Figure 7

Fibrosis in WT, Nrf2tKO, mdx and Nrf2tKOmdx hind limb muscles. (A) Tgfβ1, (B) Col1a1 levels in GM; qRT-PCR; n=9-11. (C) Representative photos and (D) semi-quantitative analysis of collagen deposition in GM

based on Masson's trichome staining; n=3-5. The data are presented as mean +/- SEM; *p≤0.05; ***p≤0.001; ****p≤0.0001. The scale bars represent 100 μm.

Fig. 8.

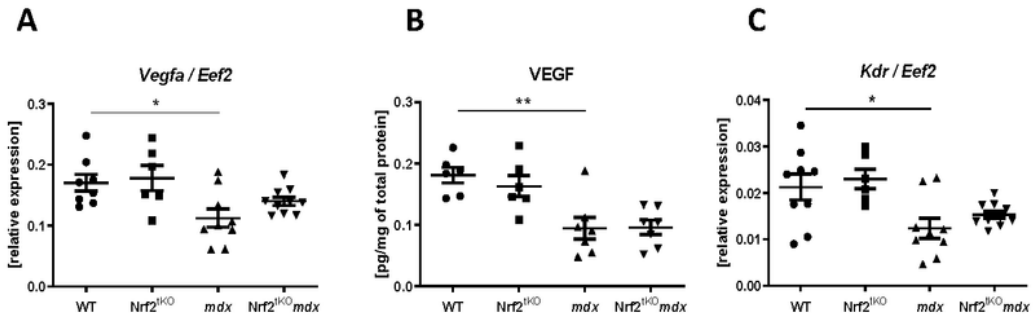

Figure 8

Expression of angiogenic mediators in skeletal muscle of WT, Nrf2tKO, mdx and Nrf2tKOmdx mice. (A) The expression of Vegfa in GM; qRT-PCR; n= 6-10 and (B) VEGF protein level in GM, LuminexTM; n= 6-7.

(C) The expression of Vegfa receptor (Kdr); qRT-PCR; n= 6-10. The data are presented as mean ± SEM. *p≤0.05; **p≤0.01.

Fig. 9.

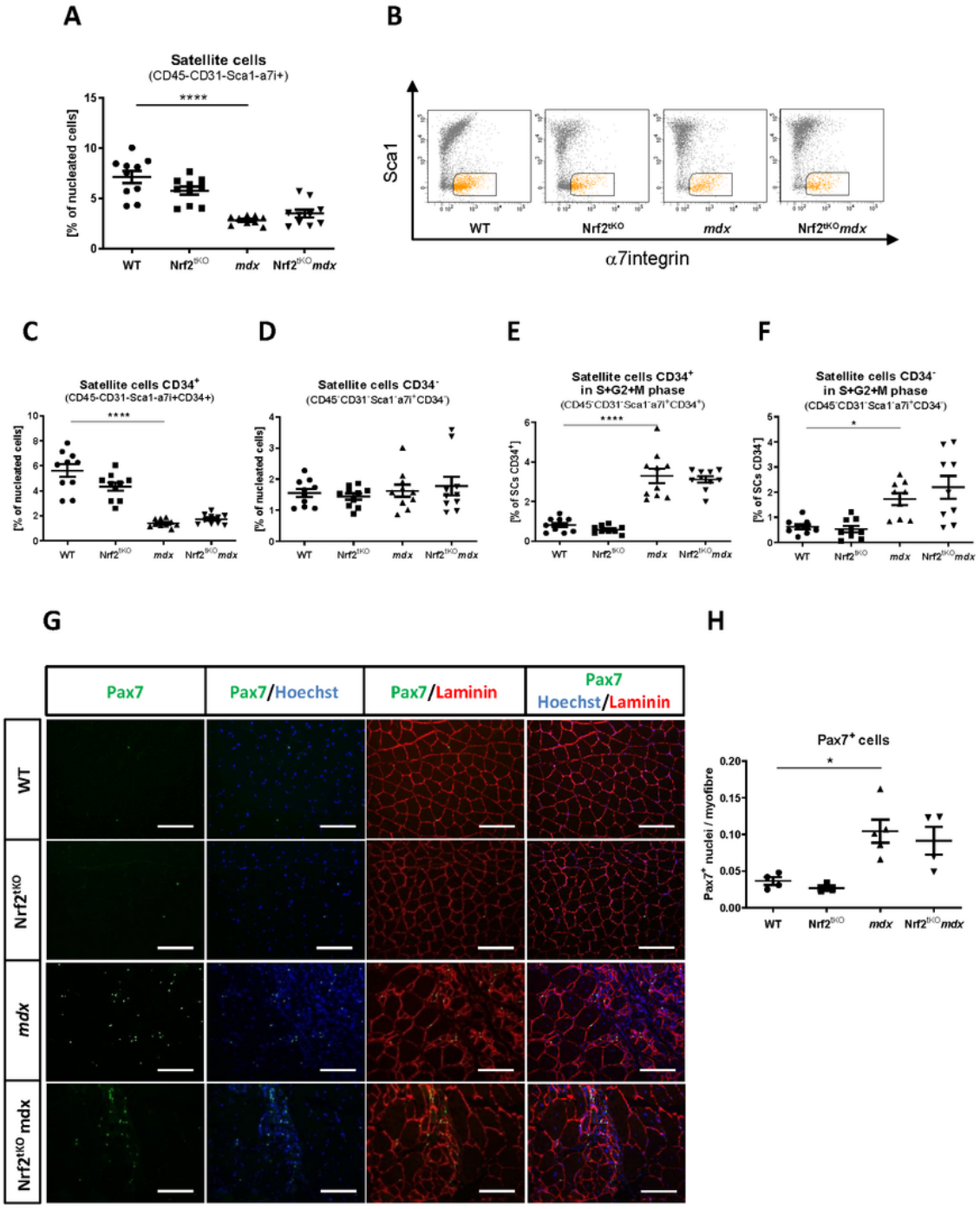

Figure 9

Number and proliferation of SCs from WT, Nrf2tKO, mdx, and Nrf2tKOmdx hind limb muscles. (A) Percentage of SCs (CD45-CD31-Sca1-α7integrin+); flow cytometry; (B) gating strategy; n=10. (C) Percentage of quiescent SCs (CD45-CD31-Sca1-α7integrin+CD34+) and (D) activated SCs (CD45-CD31-

Sca1-7integrin+CD34-); flow cytometry; n=10. (E) Percentage of proliferating SCs (CD45-CD31-Sca1-7integrin+CD34+) and (F) (CD45-CD31-Sca1-7integrin+CD34-); flow cytometry; n=10. (G) Pax7 staining in GM; representative photos. (H) Quantification of the ratio of Pax7+ cells among the total myofibers number; n=3-5. The data are presented as mean +/- SEM; *p≤0.05; ****p≤0.0001. The scale bars represent 100 µm.

Fig. 10.

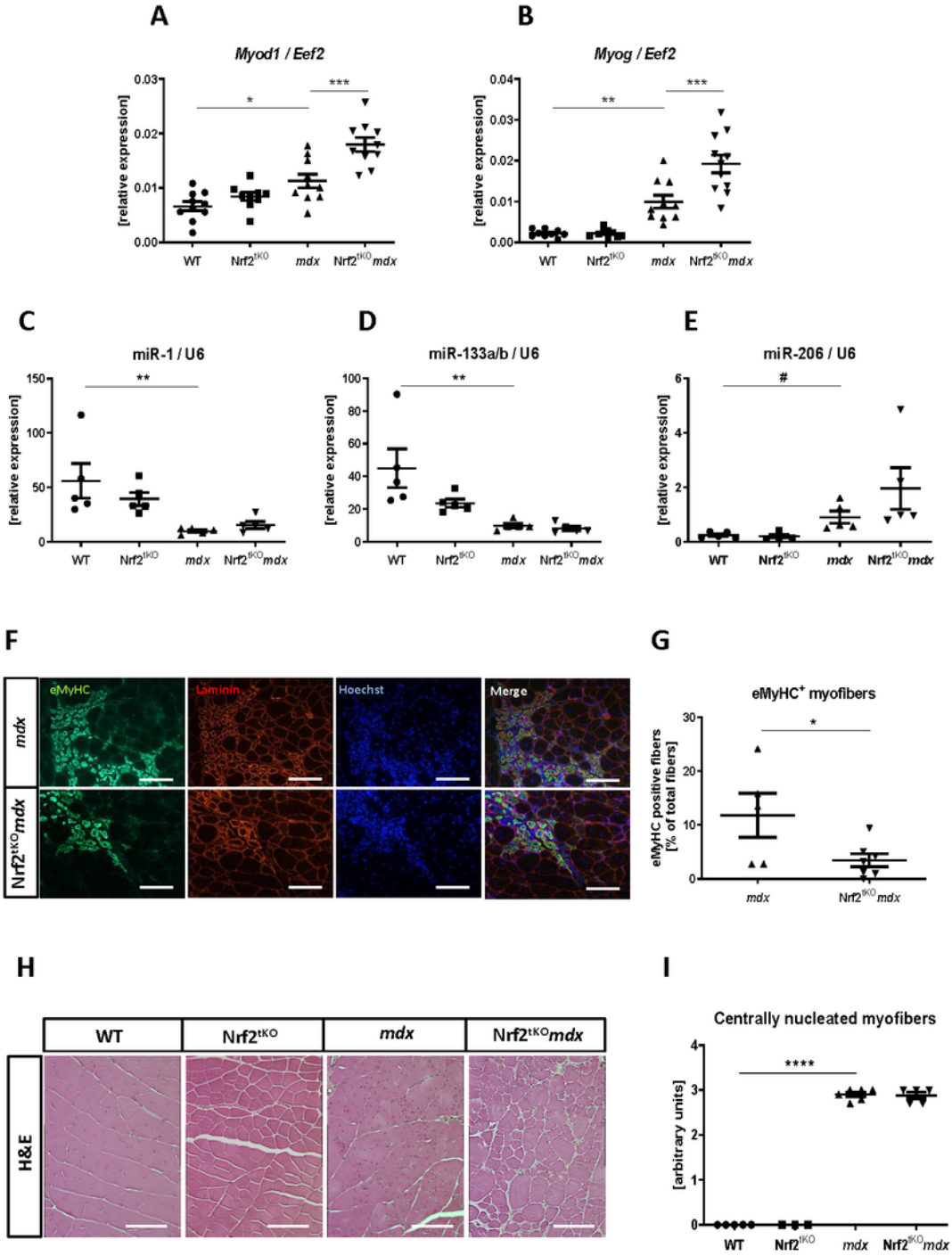

Figure 10

Regeneration of GM of WT, Nrf2tKO, mdx and Nrf2tKOmdx mice. (A) Myod1, (B) Myog, (C) miR-1, (D) miR-133a/b, (E) miR-206 level in GM; qRT-PCR; n= 9-11. (F) Representative photos of immunofluorescent staining for eMyHC and (G) quantification of the percentage of eMyHC positive myofibers; n=5-7. (H) Representative photos and (I) semi-quantitative analysis of centrally nucleated myofibers in gastrocnemius muscles based on H&E staining; n=3-6. The data are presented as mean +/- SEM; *p≤0.05; **p≤0.01; ***p≤0.001; ****p≤0.0001, one-way ANOVA with Tukey's post-hoc test; # p≤0.05 Student's t-test. The scale bars represent 100 µm.